

A Control Method using Resonant Frequency for DC Converter

Aleksandar Vuchev, Nikolay Bankov, Angel Lichev
Department of Electrical Engineering and Electronics, Technical Faculty University of Food Technologies
26 Maritza Blvd., 4002 Plovdiv
Bulgaria
{avuchev@yahoo.com} {nikolay_bankov@yahoo.com} {angel_lichev@abv.bg}



ABSTRACT: DC converters are working with resonant frequency and we use the bidirectional series DC converter in this work. We have suggested a control method by providing control characteristics improvement and decrease of the losses of the circuit elements. Using the set of existing analysis, we have introduced the improvements of the converters.

Keywords: Bidirectional Converter, Series Resonant DC-DC Converter, Control Characteristics, Efficiency

Received: 24 January 2021, Revised 31 May 2021, Accepted 21 June 2021

Copyright: Technical University of Sofia

1. Introduction

The bidirectional series resonant DC-DC converters are far well-known [1]. They hold a lot of advantages one of which are the low switching losses. During operation above the resonant frequency similarly to the other series resonant converters, their power switches are able to commute at zero voltage (ZVS) [2].

Recently, the use of bidirectional converters have become more and more popular, for example, in the hybrid renewable source energy systems [3]. In such application, they allow optimization of the energy sources operation [4] and of the system as a whole.

In [5], an analytical modeling of the resonant tank processes of a bidirectional DC-DC converter operating above the resonant frequency is presented. As a result, load and control characteristics at phase-shift control are obtained in [6]. The investigation shows that the converter behaves as an ideal current source independently from the energy flow direction. Moreover, it is able to operate without violating the ZVS conditions in a wide range of control parameter variation. Two major drawbacks are also observed. Firstly, the control characteristics hold a considerable nonlinearity. Secondly, the losses in the converter elements are significant even in no-load mode.

In the following paperwork, a different control method is proposed for compensation of the bidirectional series resonant DC-DC converter disadvantages pointed out.

2. Converter with a Phase-shift Control

Figure 1 presents the circuit of the examined converter. It consists of two identical full-bridge inverter stages, a resonant tank (L , C), a matching transformer Tr , capacitive input and output filters (C_d and C_0). Figure 1 also shows the snubber capacitors $C_1 \div C_8$ via which ZVS is obtained.

A voltage U_d is applied to the DC terminals of the “input” inverter (transistors $Q_1 \div Q_4$ with freewheeling diodes $D_1 \div D_4$), and a voltage U_0 is applied to those of the “output” one (transistors $Q_5 \div Q_8$ with freewheeling diodes $D_5 \div D_8$).

The converter operation is discussed in [5] where the possible operating modes are determined. The first of them is called **DIRECT MODE**. In this mode, it is assumed that the energy flows from the U_d to the U_0 voltage source. During the second one – the **REVERSE MODE**, the energy flows backwards – from U_0 to U_d .

Waveforms illustrating the converter operation in **DIRECT MODE** are presented in figure 2.

The “input” inverter generates the u_{ab} voltage which has a rectangular shape and a magnitude of U_d . The “output” inverter generates the u_{cd} voltage which also has a rectangular shape and a magnitude of U_0 . This voltage is phase-shifted from u_{ab} at an angle δ . At $\delta < \pi$, **DIRECT MODE** is observed, and at $\delta > \pi$ – **REVERSE MODE** is observed. Thus, the output power control is achieved by variation of the phase shift δ .

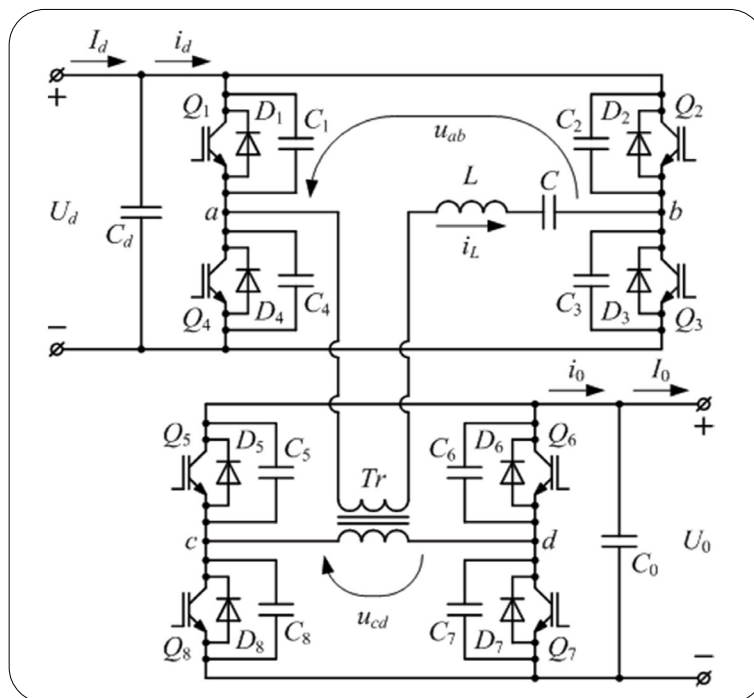


Figure 1. Circuit of the bidirectional resonant DC/DC converter

Angle φ corresponds to the “input” stage reverse diodes interval of conduction, and angle α – to the “output stage” transistors interval of conduction. The converter operates at a constant frequency ω_s higher than the resonant ω_0 . Angles φ , α and δ are measured with respect to the operating frequency ω_s .

3. Results of the Theoretical Analysis

For the purposes of the analysis, the following assumptions are made: all the circuit elements are ideal, the transformer Tr has a

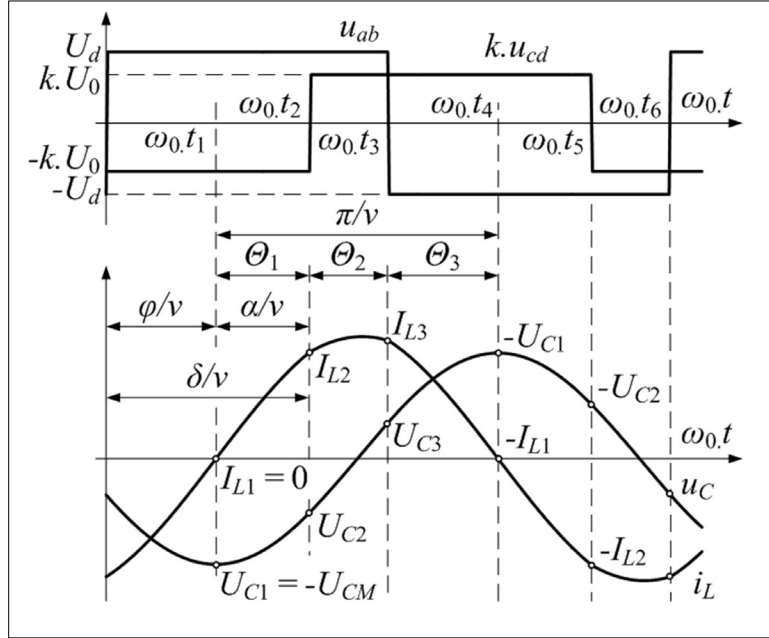


Figure 2. Waveforms at **DIRECT MODE**

ratio k , the commutations are instantaneous, and the ripples of the voltages U_d and U_0 negligible.

The analysis in [5] shows that, independently from the converter operating mode, any half period can be divided into three intervals (Figure 2). For each of these intervals, a constant equivalent voltage U_{EQ} is applied to the resonant tank. Figure 2 also presents the initial values ($I_{L1} \div I_{L3}$, $U_{C1} \div U_{C3}$) of the inductor L current i_L and the capacitor C voltage u_C for each of the intervals mentioned.

In accordance with the assumptions made, the resonant frequency, the characteristic impedance and the frequency detuning are as follows:

$$\omega_0 = 1/\sqrt{LC}; \rho_0 = \sqrt{L/C}; v = \omega_s / \omega_0 \quad (1)$$

In order to obtain generalized results, all magnitudes are normalized as follows: the voltages with respect to U_d , and the currents – with respect to U_d/ρ_0 . For each of the intervals mentioned, the normalized values of the inductor L current i'_L and the capacitor C voltage u'_C are defined as:

$$\begin{aligned} i'_{Lj}(\theta) &= I'_{Lj} \cos\theta - (U'_{Cj} - U'_{EQj}) \sin\theta \\ u'_{Cj}(\theta) &= I'_{Lj} \sin\theta + (U'_{Cj} - U'_{EQj}) \cos\theta + U'_{EQj} \end{aligned} \quad (2)$$

where j is the interval number; I'_{Lj} and U'_{Cj} are normalized values of the inductor current and the capacitor voltage at the interval beginning; $\theta = 0 \div \Theta_j$; Θ_j – interval angle with respect to the resonant ω_0 ; U'_{EQj} – normalized values of the voltage applied to the resonant tank during the interval.

Figure 2 and Figure 3 show that the value of i'_L at the end of given interval appears to be the initial value for the following one. The same is for the voltage u'_C . Therefore:

$$\begin{aligned} I'_{Lj+1} &= I'_{Lj} \cos\Theta_j - (U'_{Cj} - U'_{EQj}) \sin\Theta_j \\ U'_{Cj+1} &= I'_{Lj} \sin\Theta_j + (U'_{Cj} - U'_{EQj}) \cos\Theta_j + U'_{EQj} \end{aligned} \quad (3)$$

The interval at which $I'_{L1} = 0$ and $U'_{C1} = -U'_{CM}$ is assumed to be first. Then, the initial current (I'_{L2} and I'_{L3}) and voltage values (U'_{C2} and U'_{C3}) for the second and the third interval are calculated on the base of equations (3). The necessary for this purpose parameters Θ_j and U'_{EQj} for a half period are presented in Table 1.

MODE	Parameter	Number of interval		
		1	2	3
DIRECT	Θ_j	$\frac{\delta - \varphi}{v}$	$\frac{\pi - \delta}{v}$	$\frac{\varphi}{v}$
	U'_{EQj}	$1 + kU'_0$	$1 - kU'_0$	$-1 - kU'_0$
REVERCE	Θ_j	$\frac{\pi - \varphi}{v}$	$\frac{\delta - \pi}{v}$	$\frac{\pi - \delta + \varphi}{v}$
	U'_{EQj}	$1 + kU'_0$	$-1 + kU'_0$	$-1 - kU'_0$

Table 1.

In [5], analytical expressions are obtained for determination of the voltages U'_0 and U'_{CM} normalized values which also depend on the control parameter δ and the angle φ :

$$U'_0 = \frac{1}{k} \frac{\sin\left(\frac{\pi - \varphi}{v}\right) - \sin\left(\frac{\varphi}{v}\right)}{\sin\left(\frac{\pi - \delta + \varphi}{v}\right) - \sin\left(\frac{\delta - \varphi}{v}\right)} \quad (4)$$

$$U'_{CM} = 2 \frac{\sin\left(\frac{\varphi}{v}\right) + U'_0 \sin\left(\frac{\pi - \delta + \varphi}{v}\right)}{\sin\left(\frac{\pi}{v}\right)} - (1 + kU'_0) \quad (5)$$

In [6], expressions for determination of the normalized average values of the converter circuit currents are obtained. For example, for the **DIRECT MODE**, the output current can be determined as:

$$I'_0 = \frac{kV}{\pi} \left[I'_{L1} \sin \Theta_1 - (U'_{C1} - U'_{EQ1}) (1 - \cos \Theta_1) \right] - \frac{kV}{\pi} \sum_{j=2}^3 \left[I'_{Lj} \sin \Theta_j - (U'_{Cj} - U'_{EQj}) (1 - \cos \Theta_j) \right] \quad (6)$$

By using expressions (3) ÷ (6), values for U'_0 and I'_0 can be calculated for a fixed value of the control δ and variation of the angle φ . On the base of these values, output and control characteristics of the converter can easily be built [6].

The theoretical analysis shows that the output voltage does not depend on the output current. Therefore, the converter behaves as an ideal current source. Moreover, the output voltage does not change its polarity and can significantly exceed the input voltage independently from the energy flow direction. However, at values of the control parameter in the range $-\pi/2 \leq \delta \leq +\pi/2$, the converter ZVS operation area is very limited.

4. Improvement of the Characteristics

Exemplary control characteristics of the converter are presented in figure 3. They are obtained for different values of the frequency detuning v at $U'_0 = 1$ and $k = 1$. The characteristics show that the converter has unlimited ZVS operation with variation

of the control parameter in the range $\pi/2 \leq \delta \leq 3\pi/2$, changing both the magnitude and the direction of the transferred energy. The nonlinearity of these characteristics can be pointed out as a disadvantage.

Applying a combined control, this drawback can be corrected. Figure 4 presents a “conventional” control characteristic for the **DIRECT MODE** (with thick line). It is obtained at $U'_0 = 1, k = 1, v = \text{const} = 1,15$ and variation of the control angle in the range $\pi/2 \leq \delta \leq \pi$. Additionally, a new desired linear characteristic is presented (with dotted line), defined by the two limit states – at maximum output current value ($\delta = \pi/2$) and at idle mode ($\delta = \pi$).

A point A_1 of the first characteristic corresponds to a value of the angle $\delta = \delta_A$ at which the output current value is I'_{01} . point A_2 is obtained on the desired characteristic again for value of the angle $\delta = \delta_A$. Now the output current has a smaller value $I'_{02} < I'_{01}$. It is known that when a series-resonant converter operates above the resonant frequency its output current value can be reduced via increase of the operating frequency ω_s , in this case – the frequency detuning v . Only at $\delta = \pi/2$ the frequency is one and the same for both the old and the new characteristics.

For variation of the control angle in the range $\pi/2 \leq \delta \leq \pi$, by the use of iteration procedure, the necessary variation of the detuning v is determined. Figure 5 presents several such dependences obtained from the “conventional” control characteristics at different values of the detuning v . They are monotonously increasing and have small nonlinearity. It can be observed that in order to obtain the desired linear control characteristic, the detuning has to be altered with the angle δ increase from a minimum v_{min} to a maximum value v_{max} . For example, $v_{max} = 1,27178$ is obtained for $v_{min} = 1,15$.

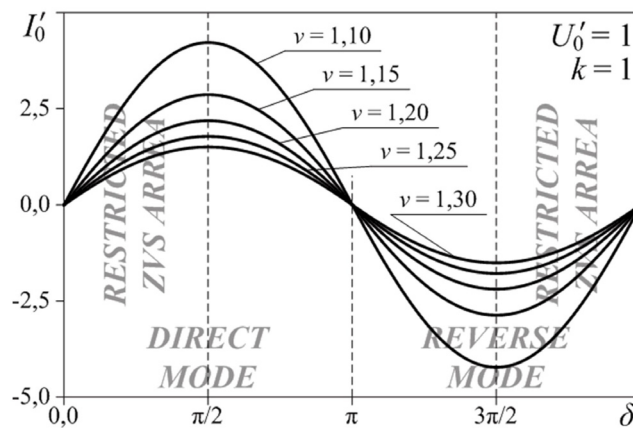


Figure 3. The phase-shift control characteristics

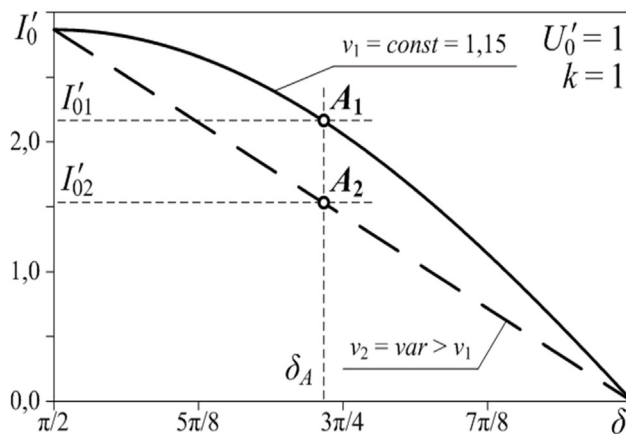


Figure 4. The control characteristic correction at **DIRECT MODE**

Because the control characteristic is symmetrically located in relation to $\delta = \pi$, a similar solution is achieved for **REVERSE MODE**.

In order to realize the desired linear control characteristic of the converter, a normalized control variable σ is introduced with range from 0 to 1. By this variable two parameters will be altered together – the angle δ and the frequency detuning v :

$$\delta = (1 + 2\sigma)\pi/2 \tag{7}$$

$$v = \begin{cases} v_{\min} + \sigma(v_{\max} - v_{\min}), & \sigma \leq 0,5 \\ v_{\min} + (1 - \sigma)(v_{\max} - v_{\min}), & \sigma > 0,5 \end{cases} \tag{8}$$

For **DIRECT MODE** $\sigma \leq 0,5$ and for **REVERSE MODE** $\sigma > 0,5$.

Although the dependence of the frequency detuning v on the control parameter σ is nonlinear, the linear approximation from (8) provides a very good result. This is demonstrated in Figure 6 where a “conventional” control characteristic is compared to one obtained from expressions (4) ÷ (8).

The proposed control method provides another advantage – the losses in the converter circuit elements are decreased. For example the RMS value I_{L_RMS} of the inductor L current decreases. The normalized expression for this value is:

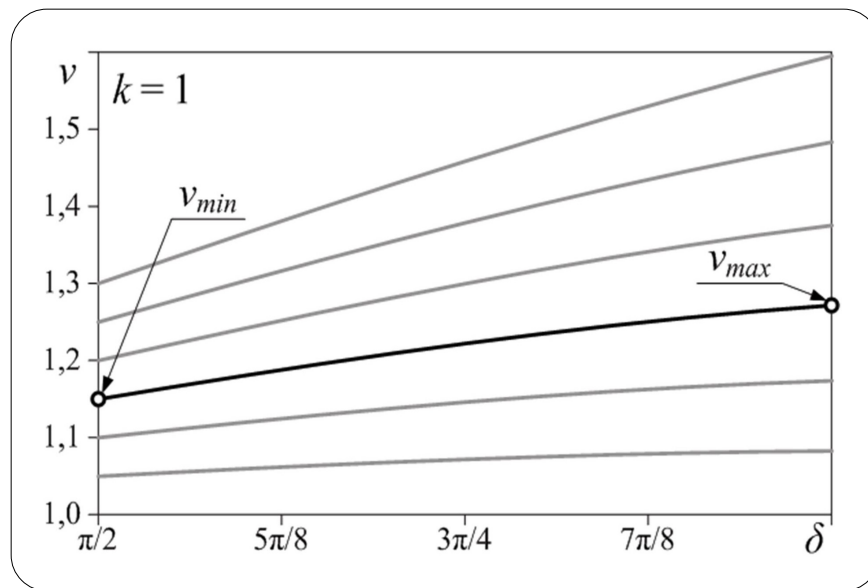


Figure 5. The wanted variation of the frequency distraction

Figure 7 presents normalized dependencies of the inductor L current on the output voltage. They are obtained for the “classical” control method – constant frequency operation ($v = 1,15$) and different values of the control angle δ . It can be observed that the inductor current increases with the decrease of the load, having greatest values at no-load mode ($\delta = \pi$).

Figure 8 presents the same dependences as the ones from figure 7. They are obtained for the “new” control method – simultaneous variation of the operating frequency and the angle δ . The maximum load characteristic ($\sigma = 0$; $\sigma = 1$) is the same as the one in figure 7. Now the load decrease leads to decrease of the inductor current, which has lowest values at no-load mode ($\sigma = 0,5$). This fact shows that the inductor losses are decreased.

It is easy to prove that this is valid for all other elements of the converter circuit.

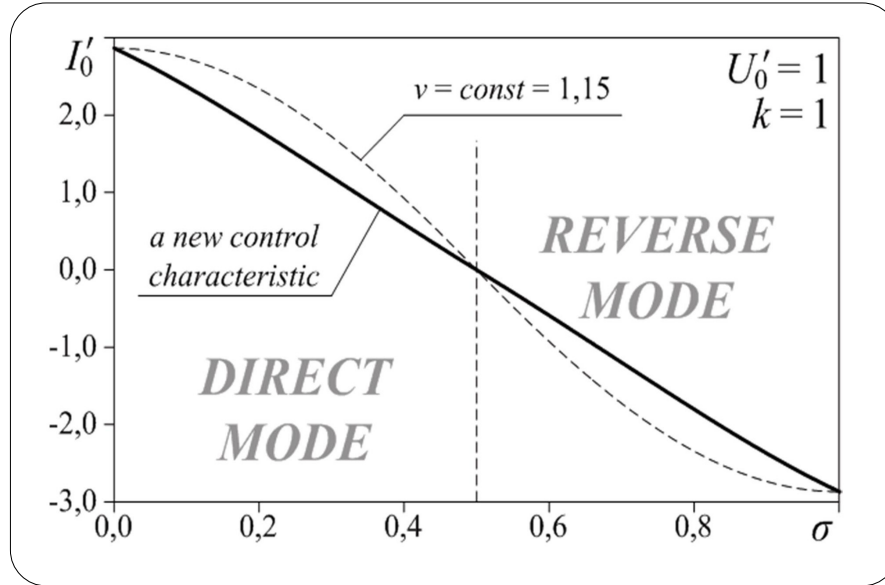


Figure 6. The corrected control characteristic

$$I'_{L_RMS} = \frac{v}{\pi} \sqrt{\left[\sum_{i=1}^3 \left(\frac{I'_{Li}}{2} \right)^2 (2\Theta_i + \sin 2\Theta_i) + \sum_{i=1}^3 \left(\frac{U'_{Ci} - U'_{EQi}}{2} \right)^2 (2\Theta_i - \sin 2\Theta_i) + \sum_{i=1}^3 I'_{Li} \frac{U'_{Ci} - U'_{EQi}}{2} (\cos 2\Theta_i - 1) \right]} \quad (9)$$

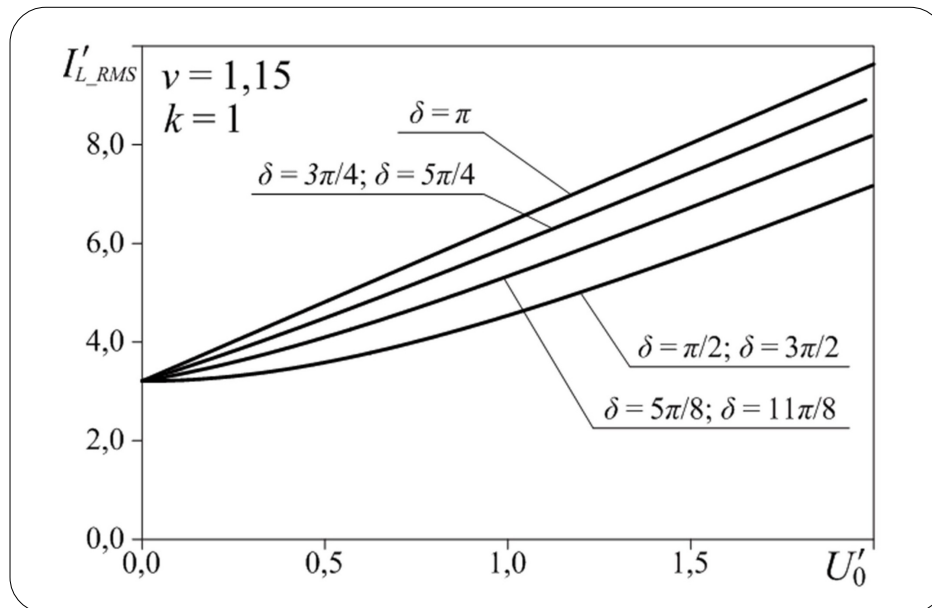


Figure 7. Normalized dependencies of the inductor current RMS value versus the output voltage at constant frequency

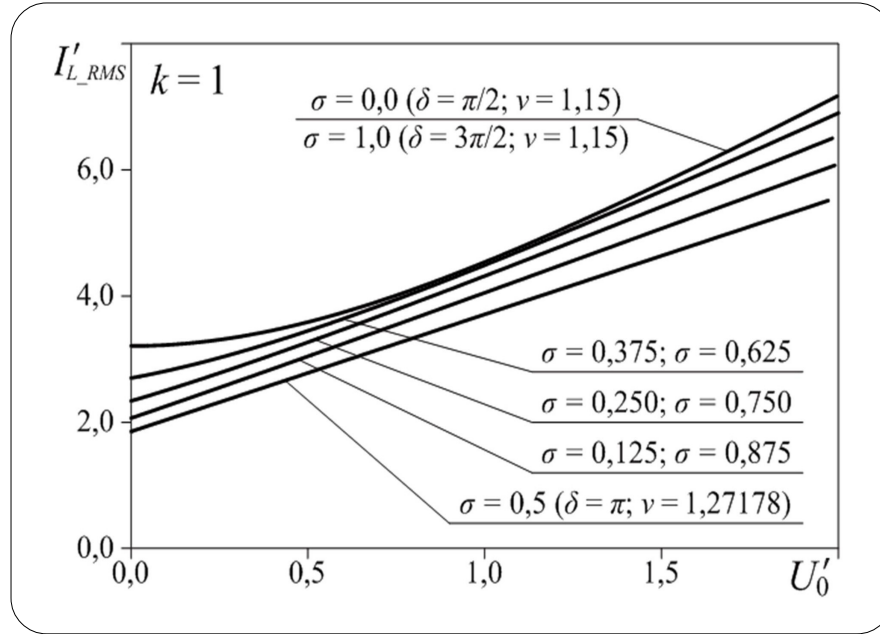


Figure 8. Normalized dependencies of the inductor current RMS value versus the output voltage at the new control method

5. Conclusion

A theoretical examination of a bidirectional series-resonant DC-DC converter operating above the resonant frequency is presented. The investigation shows two important disadvantages of the considered converter which can be significantly compensated changing the control method. It is offered the classical phase-shift control to be combined with a proportional operating frequency variation.

The new solution allows linearization of the control characteristics. In addition, the losses in the converter circuit elements are decreased.

The obtained results can be used for design of control system for bidirectional series-resonant DC-DC converters.

References

- [1] Cheron, Y., Foch, H., Roux, J. (1986). Power Transfer Control Methods in High Frequency Resonant Converters, *PCI Proceedings*, June 1986, Munich, p. 92-103.
- [2] Liu, Y., Sen, P. C. (1996). Source Reactance Lossless Switch (SRLS) for Soft-Switching Converters with Constant Switching Frequency, *IEEE Transaction on Circuits and Systems*, 1. Fundamental Theory and Applications, vol. 43, p. 301- 312.
- [3] Negi, S., Mathew, L. (2014). Hybrid Renewable Energy System: A Review, *IJEEEE*, 7 (5) 535-542.
- [4] Kotak, V. C., Tyagi, P. (2013). DC To DC Converter in Maximum Power Point Tracker, *IJAREEIE*, 2 (12) 6115- 6125, (December).
- [5] Vuchev, A., Bankov, N., Madankov, Y., Lichev, A. (2016). Analytical Modeling of a ZVS Bidirectional Series Resonant DC-DC Converter, *LIICEST*, 28-30 June 2016, Ohrid, p. 273-276.
- [6] Vuchev, A., Bankov, N., Madankov, Y., Lichev, A. (2016). Load and Control Characteristics of ZVS Bidirectional Series Resonant DC-DC Converter, *LIICEST*, 28-30 June 2016, Ohrid, p. 277-280.